*J. Am. Chem. Soc.* **1993,** *115,* 5589–5599

# Stereochemical Control of Reactivity in Co(III) Alkyl Complexes of the Tropocoronand Ligand System

**B. Scott Jaynes, Tong Ren, Axel Masschelein, and Stephen J. Lippard***

*Contribution from the Department of Chemistry, Massachusetts Institute of Technology, Cambridge, Massachusetts 02139*

*Received January 22, 1993*

**Abstract:** Reduction of the macrocyclic $Co^{II}N_4$ complexes [Co(TC-3,3)] and [Co(TC-3,4)] with 40% Na/Hg followed by addition of alkyl halide gave the five-coordinate diamagnetic Co(III) alkyl compounds, [CoR(TC-3,3)] (R = Me, Et, *n*-Pr) and [Co(*n*-Pr)(TC-3,4)]. Addition of MeLi to a cold THF solution of [CoCl(TC-4,4)] yielded the five-coordinate complex [CoMe(TC-4,4)]. X-ray structural analyses of [CoR(TC-3,3)] (R = Et, *n*-Pr) and [CoMe(TC-4,4)] revealed that both complexes have square-pyramidal coordination geometries. This result may be contrasted with the finding that the structures of the corresponding [CoCl(TC-*n*,*n*)] complexes change from square pyramidal to trigonal bipyramidal as *n* changes from 3 to 4. Square-pyramidal stereochemistry for [CoMe(TC-4,4)] is attributed to the stronger $\sigma$-donating character of the methyl group compared to chloride ion. All three Co(III) alkyl complexes homolyze in solution in room light, or at elevated temperatures in the dark, to afford the corresponding Co(II) tropocoronand complex and alkyl radical. The Co–C bond in [CoMe(TC-4,4)] homolyzes more than 13 times faster than that in [CoMe(TC-3,3)], reflecting the torsional strain within the methylene linker chains of the ligand. Significantly, [CoMe(TC-4,4)] reacts rapidly with 1–2 atm of CO at 40 °C to yield the CO insertion product [Co(COMe)(TC-4,4)], whereas [CoEt(TC-3,3)] does not react with CO under identical conditions. An X-ray structural study revealed that the acyl complex is five coordinate, with a stereochemistry that is between square pyramidal and trigonal bipyramidal. This structure further displays the dual control of metal geometry by the steric constraints of the tropocoronand and the donor property of the fifth ligand. CO insertion probably proceeds for [CoMe(TC-4,4)] because the more flexible $[TC\text{-}4,4]^{2-}$ ligand affords a coordination site cis to the methyl group to which the CO can transiently bind.

## Introduction

Coenzyme $B_{12}$ (cobalamin) has attracted the attention of organic, inorganic, and biological chemists since the structure determination of its vitamin form in the 1950's and of the coenzyme itself in the early 1960's.[1] Adenosylcobalamin serves as a source of adenosyl radicals, formed in the homolysis of the Co–C bond, which are subsequently utilized by certain enzymes to carry out transformations of the general form illustrated in eq 1. A radical generated by interaction of the enzyme/substrate complex with the coenzyme abstracts a hydrogen atom from the substrate, the resulting radical is exchanged with a neighboring functional group X on the substrate, and the H atom is returned to regenerate the adenosyl radical.[2] The net result for the substrate is catalytic 1,2-exchange of X with hydrogen on an adjacent carbon atom. Enzymes that utilize radicals formed by the homolysis of adenosylcobalamin include methylmalonyl-CoA mutase, diol dehydrase, and ethanolamine ammonia lyase.[3]

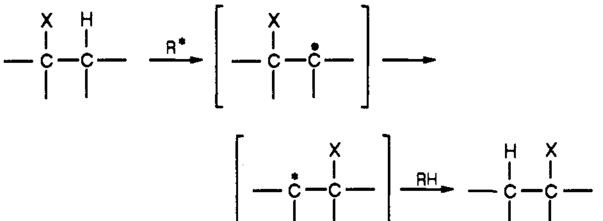

(1)

Although the biological function of adenosylcobalamin is well understood, the mechanism of the homolysis of the Co–C bond is still in question. The Co–C bond dissociation energy of the coenzyme has been determined to be 26–31 kcal/mol[4,5] and, although relatively weak compared to a typical C–C bond, the rate of homolysis of the bond at 25 °C in water is only $10^{-9}$ $s^{-1}$.[6] Activation of the Co–C bond by the enzyme and substrate, however, has been estimated to enhance the rate of homolysis by approximately $10^{11}$ over the rate observed for adenosylcobalamin alone.[6] The manner by which the enzyme or enzyme/substrate complex accelerates this rate is not understood, but increasing evidence suggests that steric interactions between the corrin ring and the adenosyl moiety may weaken the Co–C bond upon binding of the enzyme.

The concept of physical distortion of the coenzyme by the enzyme was proposed as early as 1969,[7] but little evidence supporting such a theory was available until the 1980's. Model studies by Halpern using Co alkyl complexes of the dimethylglyoxime ligand system, $CoR(DH)_2L$, revealed that, by increasing the steric bulk of axial phosphine ligands (L), the Co–C bond on the opposite side of the ring is weakened.[2] Since both dimethylglyoxime and the corrin ring are relatively flexible systems, these observations were taken as evidence that enzyme binding may similarly weaken the Co–C bond in $B_{12}$ by forcing steric interactions between the corrin ring substituents and the adenosyl group.

More direct evidence for steric activation of the Co–C bond was provided by studies of the neopentylcobalamin system in which the adenosyl group of the coenzyme is replaced by a bulky neopentyl group. Chemaly and Pratt, who first synthesized this complex, as well as subsequent investigators found that its Co–C bond is unusually labile to homolysis,[8] presumably because of steric interactions between the neopentyl group and the corrin ring substituents. Finke has recently reported that neopentyl-

---

(1) Glusker, J. P. In *B₁₂*; Dolphin, D., Ed.; John Wiley and Sons: New York, 1982; Vol. 1, pp 23–106.

(2) Halpern, J. *Science* **1985**, *227*, 869.

(3) Golding, B. T. In *B₁₂*; Dolphin, D., Ed.; John Wiley and Sons: New York, 1982; Vol. 1, pp 543–582.

(4) Finke, R. G.; Hay, B. J. *Inorg. Chem.* **1984**, *23*, 3041.

(5) Halpern, J.; Kim, S.-H.; Leung, T. W. *J. Am. Chem. Soc.* **1984**, *106*, 8317.

(6) Hay, B. P.; Finke, R. G. *J. Am. Chem. Soc.* **1987**, *109*, 8012.

(7) Hill, H. A. O.; Pratt, J. M.; Williams, R. J. P. *Chem. Brit.* **1969**, *5*, 156.

0002-7863/93/1515-5589$04.00/0

cobalamin homolyzes $10^6$ times faster than the adenosyl derivative.[9] This relative rate enhancement is the largest yet observed for $B_{12}$ or a $B_{12}$ model system in the absence of an enzyme and further indicates that steric interactions may provide a substantial part of the rate acceleration of the enzymes.

The tropocoronands are tetraaza dianionic macrocyclic ligands that are similar in some respects to the corrin and porphyrin ring systems.[10] We have investigated four-coordinate Co(II) and five- and six-coordinate Co(III) tropocoronand complexes and found their geometry to be strongly dependent on the size of the macrocycle.[11] The complexes twist as the length of the flexible methylene linker chains increases because of increasing torsional strain. In the case of the five-coordinate Co(III) halide complexes, the geometry varies from square pyramidal for [CoCl(TC-3,3)] to trigonal bipyramidal for [CoCl(TC-4,4)], a rare configuration for Co(III).[11]

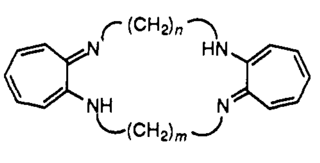

tropocoronand, $H_2$(TC-*n*,*m*)

Given these results, it was of interest to determine whether the tropocoronand ring could provide a framework for coordinating Co(III) alkyl species. We initially envisioned that the preparation of cobalt alkyl tropocoronands with macrocycles of varying size would afford coenzyme $B_{12}$ model systems with adjustable steric environments that were controlled independently from the choice of axial ligands. In particular, we wished to examine the effects of a $D_{2d}$ twist of the $CoN_4$ plane. Here we report the synthesis and spectroscopic characterization of Co(III) alkyl complexes of $[TC\text{-}3,3]^{2-}$ $[TC\text{-}3,4]^{2-}$, and $[TC\text{-}4,4]^{2-}$, as well as the X-ray structures of [CoEt(TC-3,3)], [Co(*n*-Pr)(TC-3,3)], and [CoMe(TC-4,4)]. The Co–C bond was found to be thermally and photochemically labile, as in other $B_{12}$ model complexes. In contrast to the Co(III) halides, the five-coordinate alkyl complexes have square-pyramidal coordination geometries which are nearly independent of the size of the ligand, possible explanations for which are discussed. Despite their stereochemically similar coordination spheres, the [CoR(TC-3,3)] and [CoR(TC-4,4)] alkyl complexes differ substantially in their bond homolysis rates and ability to undergo CO insertion. These differences in reactivity are ascribed to the varying degree of stereochemical constraint of the two ligands. An X-ray structural characterization of the [Co($COCH_3$)(TC-4,4)] acyl complex is also presented.

## Experimental Section

**General Information.** Diethyl ether, pentane, tetrahydrofuran (THF), and toluene were distilled from sodium benzophenone ketyl under nitrogen. $H_2$(TC-*n*,*m*) (*n*,*m* = 3,3; 3,4; 4,4),[12] [Co(TC-3,3)], [Co(TC-3,4)], [Co(TC-4,4)], and [CoCl(TC-4,4)] were prepared as reported previously.[11] MeLi (1.4 M in diethyl ether) and MeMgBr (1.4 M in 75% toluene/25% THF) (Aldrich) were used as received. MeI was obtained from Aldrich, passed through a short column of alumina, and distilled prior to use. EtBr and *n*-PrBr from commercial vendors were dried over 4 Å molecular sieves and distilled prior to use. 2,2,6,6-Tetramethylpiperidine-1-oxyl (TEMPO) was purchased from Aldrich and purified by sublimation. The 40% Na/Hg was prepared under inert atmosphere by adding the mercury dropwise to molten sodium and allowing the solution to cool to room temperature. "Ultra high purity" grade carbon monoxide from Matheson was used as received. All experiments were carried out either in a nitrogen-filled Vacuum Atmospheres glovebox or with the use of conventional Schlenk line techniques under purified argon. Infrared spectra were recorded on either a Mattson Cygnus 100 Fourier transform or a Bio-Rad FTS 7 Fourier transform instrument. UV–visible spectra were recorded on either a Perkin-Elmer Lambda 7 or a Hewlett Packard 8452A diode array spectrophotometer. NMR spectra were recorded on a Varian XL-300 at room temperature unless otherwise noted.

**Synthetic Procedures. Light Sensitivity.** Cobalt(III) alkyl tropocoronand solutions are light sensitive at room temperature, but they can be handled in very dim room light for brief periods. Crystalline samples showed no photosensitivity under an inert atmosphere.

**[CoEt(TC-3,3)].** A solution of [Co(TC-3,3)] (32.2 mg, 0.085 mmol) in 5 mL of THF was treated with 4 drops of 40% Na/Hg and stirred rapidly. After approximately 10 min, the dark green-black solution turned vivid blue-green, indicating that reduction to Co(I) had occurred. The blue-green solution was filtered through a glass frit, which was pre-rinsed with rigorously dry THF, and cooled to −30 °C. Under dim light, EtBr (9.5 μL, 0.127 mmol) was added to the cold solution by syringe causing an immediate color change to brown. The solution was stirred for 3 min at room temperature, after which time the solvent was removed under reduced pressure. The resulting brown solid was dissolved in 4 mL of toluene, and then the solution was filtered through a frit, layered with 2 mL of pentane, and stored at −30 °C. Black needle-shaped crystals formed overnight which were collected and rinsed with a small amount of pentane (11 mg, 32%). Crystals suitable for X-ray structural determination were grown by slow diffusion of pentane into a dichloromethane solution of the product at −30 °C. $^1H$ NMR ($d_8$-toluene) δ 6.66 (t, 4H, *J* = 10 Hz), 6.52 (d, 4H, *J* = 11 Hz), 6.20 (t, 2H, *J* = 9 Hz), 3.10 (m, 8H), 2.18 (q, 2H, *J* = 8 Hz), 1.87 (m, 2H), 1.76 (m, 2H), −0.54 (t, 3H, *J* = 8 Hz). UV–vis (THF) [$\lambda_{max}$, nm ($\epsilon_M$, cm$^{-1}$ M$^{-1}$)] 411 (35 700), 801 (10 400). FTIR (KBr, cm$^{-1}$) 1574 (s), 1498 (s), 1403 (s), 1275 (m), 1226 (s), 1143 (w), 1113 (m), 1032 (m), 964 (w), 884 (m), 714 (s), 508 (m). Anal. Calcd for $C_{22}H_{27}N_4Co$: C, 65.01; H, 6.70; N, 13.79. Found: C, 64.87; H, 6.87; N, 13.69.

**[Co(*n*-Pr)(TC-3,3)].** A solution of [Co(TC-3,3)] (33.5 mg, 0.089 mmol) in 5 mL of THF was treated with 40% Na/Hg, filtered, and cooled to −30 °C as described above for [CoEt(TC-3,3)]. Addition of *n*-PrBr (12 μL, 0.132 mmol) caused the blue-green solution to turn brown. After the mixture was stirred for approximately 3 min at room temperature, the solvent was removed under reduced pressure, the remaining solid was redissolved in 4 mL of toluene, and the solution was filtered into a vial, layered with 2 mL of pentane, and stored at −30 °C. A black crystalline solid formed overnight which was collected and rinsed with a small amount of pentane (15 mg, 40%). Crystals suitable for X-ray structural determination were grown by slow diffusion of diethyl ether into a benzene solution of the product. $^1H$ NMR ($d_8$-toluene) δ 6.66 (t, 4H, *J* = 10 Hz), 6.53 (d, 4H, *J* = 11 Hz), 6.19 (t, 2H, *J* = 9 Hz), 3.13 (t, 8H, *J* = 5 Hz), 2.16 (t, 2H, *J* = 8 Hz), 1.90 (m, 2H), 1.72 (m, 2H), 0.70 (t, 3H, *J* = 7 Hz), 0.42 (sx, 2H, *J* = 9 Hz). UV–vis (THF) [$\lambda_{max}$, nm ($\epsilon_M$, cm$^{-1}$ M$^{-1}$)] 411 (33 800), 796 (9 720). FTIR (KBr, cm$^{-1}$) 1572 (s), 1496 (s), 1405 (s), 1271 (m), 1227 (m), 1141 (w), 1107 (m), 1031 (m), 963 (w), 882 (m), 712 (s), 573 (w), 502 (m). Anal. Calcd for $C_{23}H_{29}N_4Co$: C, 65.70; H, 6.95; N, 13.33. Found: C, 66.23; H, 7.24; N, 12.92.

**[Co(*n*-Pr)(TC-3,4)].** A solution of [Co(TC-3,4)] (46.6 mg, 0.119 mmol) in 5 mL of THF was reduced with 40% Na/Hg and treated with *n*-PrBr (21.7 μL, 0.238 mmol) as described for [Co(*n*-Pr)(TC-3,3)]. Black, partially crystalline material was isolated from toluene as indicated above and rinsed with a small amount of pentane (14 mg, 27%). $^1H$ NMR ($d_8$-toluene) δ 6.60 (m, 8H), 6.23 (t, 2H, *J* = 8 Hz), 3.41 (m, 4H), 3.07 (m, 4H), 2.17 (t, 2H, *J* = 8 Hz), 2.02 (m, 2H), 1.81 (m, 2H), 1.59 (m, 2H), 0.70 (t, 3H, *J* = 7 Hz), 0.38 (sx, 2H, *J* = 8 Hz). UV–vis (THF) [$\lambda_{max}$, nm ($\epsilon_M$, cm$^{-1}$ M$^{-1}$)] 409 (29 300), 825 (6 160). Anal. Calcd for $C_{24}H_{31}N_4Co$: C, 66.35; H, 7.19; N, 12.90. Found: C, 67.05; H, 7.54; N, 12.74.

**[CoMe(TC-4,4)]. Method A.** A slurry of [CoCl(TC-4,4)] (46 mg, 0.104 mmol) was prepared in 5 mL of THF and cooled to −30 °C. MeLi (75 μL/1.4 M, 0.105 mmol) was added by syringe and the reaction was allowed to stir for approximately 3 min as it warmed to room temperature. The solvent was removed under reduced pressure leaving a brown residue. The brown solid was redissolved in 4 mL of toluene, and then the solution was filtered into a vial, layered with 1 mL of pentane, and stored at −30 °C. Black, partially crystalline solid (17 mg, 39%) was isolated after 18

---

(8) (a) Chemaly, S. M.; Pratt, J. M. *J. Chem. Soc., Dalton Trans.* **1980**, 2274. (b) Schrauzer, G. N.; Grate, J. H. *J. Am. Chem. Soc.* **1981**, *103*, 541. (c) Kim, S-H.; Chen, H. L.; Feilchenfeld, N.; Halpern, J. *J. Am. Chem. Soc.* **1988**, *110*, 3120. (d) Brown, K. L.; Brooks, H. B. *Inorg. Chem.* **1991**, *30*, 3420.

(9) Waddington, M. D.; Finke, R. G. *J. Am. Chem. Soc.* Submitted for publication.

(10) Villacorta, G. M.; Lippard, S. J. *Pure Appl. Chem.* **1986**, *58*, 1477.

(11) Jaynes, B. S.; Ren, T.; Liu, S.; Lippard, S. J. *J. Am. Chem. Soc.* **1992**, *114*, 9670.

(12) Zask, A.; Gonnella, N.; Nakanishi, K.; Turner, C. J.; Imajo, S.; Nozoe, T. *Inorg. Chem.* **1986**, *25*, 3400.

h and rinsed with a small amount of pentane. Recrystallization of the compound in toluene/pentane resulted in crystals that were suitable for X-ray structural determination. $^1$H NMR ($d_8$-toluene) $\delta$ 6.64 (t, 4H, $J$ = 10 Hz), 6.46 (d, 4H, $J$ = 11 Hz), 6.14 (t, 2H, $J$ = 9 Hz), 3.38 (m, 8H), 2.02 (m, 4H), 1.77 (s, 3H), 1.57 (m, 4H). UV–vis (THF) [$\lambda_{max}$, nm ($\epsilon_M$, cm$^{-1}$ M$^{-1}$)] 408 (26 400), 762 (4 880). FTIR (KBr, cm$^{-1}$) 1576 (s), 1502 (s), 1427 (m), 1396 (m), 1374 (m), 1332 (m), 1261 (m), 1221 (m), 1079 (w), 993 (w), 970 (w), 914 (w), 882 (w), 717 (s), 497 (w). Anal. Calcd for $C_{23}H_{29}N_4Co$: C, 65.70; H, 6.95; N, 13.33. Found: C, 65.80; H, 6.80; N, 13.27.

**Method B.** A slurry of [CoCl(TC-4,4)] (44.9 mg, 0.102 mmol) was prepared in 2 mL of toluene, cooled to −30 °C, and treated with MeMgBr (73 $\mu$L/1.4 M, 0.102 mmol). The mixture was stirred for 5 min at room temperature and then filtered into a vial. The solution was layered with 2 mL of pentane and stored at −30 °C. Black crystalline solid (13 mg, 30%) was isolated after 18 h and rinsed with a small amount of pentane. The proton NMR and UV–visible spectra were identical to those of material prepared by Method A.

**[Co(COMe)(TC-4,4)].** A slurry of [CoCl(TC-4,4)] (51.0 mg, 0.116 mmol) was prepared in 3 mL of toluene, cooled to −30 °C, and treated with MeMgBr (83 $\mu$L/1.4 M, 0.116 mmol). After the mixture was stirred for 5 min at room temperature, the flask was evacuated briefly and refilled with CO (6 psig), causing a gradual color change from black-green to dark blue-green over 1 h. The solution was then filtered into a vial, layered with 2 mL of pentane, and stored at −30 °C for 24 h. The black crystalline product (18 mg, 35%) was collected and rinsed with a small amount of pentane. Recrystallization from toluene/pentane resulted in material that was suitable for an X-ray crystal structure analysis. $^1$H NMR ($d_8$-toluene) $\delta$ 6.62 (m, 8H), 6.28 (t, 2H, $J$ = 9 Hz), 3.38 (m, 8H), 2.09 (s, 3H), 1.98 (m, 4H), 1.54 (m, 4H). UV–vis (THF) [$\lambda_{max}$, nm ($\epsilon_M$, cm$^{-1}$ M$^{-1}$)] 394 (28 600), 600 (7 000), 835 (5 520). FTIR (KBr, cm$^{-1}$) 1685 (s), 1581 (m), 1504 (s), 1448 (m), 1414 (m), 1372 (m), 1283 (m), 1259 (m), 1224 (m), 1074 (w), 721 (m). Anal. Calcd for $C_{24}H_{29}N_4OCo$: C, 64.28; H, 6.52; N, 12.49. Found: C, 64.92; H, 6.62; N, 12.20.

**1-Methoxy-2,2,6,6-tetramethylpiperidine (MeTEMPO).** This compound was prepared by a published procedure[13] with the following modifications. To a solution of 2,2,6,6-tetramethylpiperidine-1-oxyl (TEMPO) (0.416 g, 2.66 mmol) in 5 mL of diethyl ether at −78 °C was added a solution of MeMgBr (0.89 mL/1.4M, 2.67 mmol) in 5 mL of diethyl ether. The resulting mixture was quenched with 10 mL of aqueous $NH_4Cl$, washed with distilled water, and dried over $MgSO_4$. The ether solution was stripped under reduced pressure to an orange oil and then chromatographed on a 1.5 × 20 cm silica gel column using 4:1 hexane/diethyl ether as an eluant. The eluant was collected in one fraction until the orange band (TEMPO) moved nearly to the bottom of column. Removal of the solvent under reduced pressure left a pale yellow oil. $^1$H NMR ($CDCl_3$) $\delta$ 3.58 (s, 3H), 1.60–1.20 (m, 6H), 1.14 (s, 6H), 1.05 (s, 6H).

**Molecular Orbital Calculations.** All computations were carried out on a VAX-3400 workstation running VMS V5.2. The SCF-multiple scattering-X$\alpha$ program was developed by M. Cook (Harvard) and B. E. Bursten and G. C. Stanley (Texas A&M) and employed the usual methodology.[14–16] Norman's overlapping radii[17] were taken to be 88.5% of the atomic number radii with the outersphere made tangent to the outer atomic sphere. The $\alpha$ values of the atomic sphere were taken from Schwartz,[18] whereas those for both intersphere and outersphere were taken as the valence electron weighted average of the atomic $\alpha$. Since all the model compounds were dianions, a Watson sphere coinciding with an outersphere charge of +3 was used. Restricted SCF iterations were considered to be converged if the potential change was less than 0.001 Ry (Rydberg = 13.6 eV).

**Alkyl Radical Trapping Experiments.** Gas chromatography (GC) was performed on a 5890A Hewlett Packard gas chromatograph equipped with an FID detector and either a cross-linked methyl silicone (HP) or cross-linked FFAP (HP) column of dimensions 10 m × 0.5 mm × 1.0 $\mu$m. GC/mass spectra were recorded on the same instrument equipped with a 5971A Hewlett Packard mass selective detector. The initial oven temperature was held at 50 °C for 2 min and then increased at a rate of 15 °C/min to a final temperature of 200 °C.

**[CoMe(TC-3,3)] + TEMPO.** A solution of [Co(TC-3,3)] (16.6 mg, 0.044 mmol) was dissolved in 5 mL of THF and treated with 4 drops of 40% Na/Hg as described above for [CoEt(TC-3,3)]. The resulting blue-green solution was cooled to −78 °C and then MeI (5.5 $\mu$L, 0.088 mmol) was added by syringe. To this solution was added a solution of TEMPO (68.7 mg, 0.440 mmol) and ferrocene (11.4 mg, 0.061 mmol; used as a quantitation standard) in 5 mL of THF. The resulting solution was slowly warmed to 50 °C for 2 h in darkness to ensure homolysis of the Co–C bond and then the solution was analyzed by gas chromatography. A separate THF solution of ferrocene (0.0109 M) and MeTEMPO (0.014 M) was injected to calibrate the integrated GC response. The yield of MeTEMPO for the homolysis was 37%.

**[CoMe(TC-4,4)] + TEMPO.** A solution of [CoMe(TC-4,4)] (12.0 mg, 0.029 mmol), TEMPO (44.6 mg, 0.285 mmol), and ferrocene (10.4 mg, 0.056 mmol) was prepared in 8 mL of THF, sealed, and heated in darkness at 50–55 °C for 2 h. Analysis by GC as described for [CoMe(TC-3,3)] indicated a 26% yield of MeTEMPO. After the solution was stirred in room light for 1 h, the yield of MeTEMPO rose to 33%.

**Kinetic Analysis of the Co–C Bond Homolysis Reactions.** In a typical reaction, a quartz cuvette fitted with a stir bar was filled with 3.5 mL of a 5.3 mM solution of TEMPO in THF. The cuvette was sealed with a septum and equilibrated at the desired temperature. A 30-$\mu$L portion of cold Co–alkyl solution was injected through the septum and 10 to 20 s of stirring were allowed before spectra were collected. The final concentration of [CoMe(TC-*n*,*n*)] in the cell was 2.9 × 10$^{-2}$ mM, from which we compute a 181-fold excess of TEMPO over Co–alkyl. All spectra were recorded on a Hewlett Packard photodiode array spectrophotometer controlled by a Macintosh IIfx computer running software written locally for Labview2 (National Instruments).

**Solution and Refinement of Crystal Structures.** Table I summarizes the details of data collection, reduction, and refinement; typical procedures in our laboratory have been described previously.[19] All data were collected on an Enraf-Nonius CAD-4F diffractometer by using monochromated Mo K$\alpha$ ($\lambda$ 0.7107) radiation and $\omega/2\theta$ scans. Monitoring of standard reflections showed no crystal decay for any case.

**[CoEt(TC-3,3)].** A black prism-shaped crystal with dimensions 0.05 × 0.08 × 0.40 mm was mounted with silicone grease on a quartz fiber under a cold flowing stream of nitrogen. Open counter $\omega$-scans of low angle reflections revealed sharp ($\Delta\bar{\omega}_{1/2}$ = 0.25°) structureless profiles. The systematic absences were consistent with space groups $P2_1$ and $P2_1/m$, but the structure could only be solved and refined successfully in the former. The unit cell parameters were refined by using the setting angles of 25 reflections having $2\theta \geq 12°$. An empirical absorption correction was applied. The structure was solved by using standard Patterson and difference Fourier techniques and refined with anisotropic temperature factors for the non-hydrogen atoms. The hydrogen atoms were placed at fixed C–H distances of 0.95 Å at idealized geometries and constrained to ride on the respective carbon atoms. The absolute configuration was determined by refining on both enantiomers and choosing that which refined to the lowest discrepancy factors. Final coordinates for the non-hydrogen atoms are given in Table II. Positional parameters for all atoms, anisotropic temperature factors, and all bond lengths and angles appear as Tables S1–S3 (supplementary material), respectively.

**[Co(*n*-Pr)(TC-3,3)].** A black rectangular plate with dimensions 0.02 × 0.18 × 0.30 mm and bound by faces {100}, {010}, and {001} was mounted as described above for [CoEt(TC-3,3)]. Open counter $\omega$-scans of low angle reflections revealed sharp ($\Delta\bar{\omega}_{1/2}$ = 0.19°) structureless profiles. The space group was determined to be *Pccn* from the systematic absences. The unit cell parameters were refined by using the setting angles of 25 reflections having $2\theta \geq 12°$. An analytical absorption correction was applied. The structure was solved and refined as described above for [CoEt(TC-3,3)]. Final coordinates for the non-hydrogen atoms are given in Table III. Positional parameters for all atoms, anisotropic temperature factors, and all bond lengths and angles appear as Tables S4–S6 (supplementary material), respectively.

**[CoMe(TC-4,4)].** A black, block-shaped crystal with approximate dimensions 0.20 × 0.30 × 0.40 mm was mounted as described above for [CoEt(TC-3,3)]. Open counter $\omega$-scans of low angle reflections revealed sharp ($\Delta\bar{\omega}_{1/2}$ = 0.29°) structureless profiles. The space group was determined to be either $Pca2_1$ or *Pcam* from the systematic absences. Successful solution of the structure in the former indicated that it was the correct choice. In addition, the mirror plane required in the space group *Pcam* is not present in the structure. The unit cell parameters were refined by using the setting angles of 25 reflections having $2\theta \geq 22°$. An

---

[13] Hill, C. L.; Whitesides, G. M. *J. Am. Chem. Soc.* **1974**, *96*, 870.

[14] Slater, J. C. *The Self-Consistent Field for Molecules and Solids*; McGraw-Hill: New York, 1974; Vol. 4.

[15] Johnson, K. H. *Adv. Quantum Chem.* **1973**, *7*, 143.

[16] Connolly, J. W. D. In *Semiempirical Methods of Electronic Structure Calculation, Part A: Techniques*; Segal, G. A., Ed.; Plenum Press: New York, 1977.

[17] Norman, J. G. *Mol. Phys.* **1976**, *31*, 1191.

[18] Schwartz, K. *Phys. Rev.* **1972**, *5*, 2466.

[19] Carnahan, E. M.; Rardin, R. L.; Bott, S. G.; Lippard, S. J. *Inorg. Chem.* **1992**, 5193.

**Table I.** Experimental Details of the X-ray Diffraction Studies

| | [CoEt(TC-3,3)] | [Co(*n*-Pr)(TC-3,3)] | [CoMe(TC-4,4)] | [Co(COMe)(TC-4,4)] |
|---|---|---|---|---|
| formula | $\mathrm{CoC_{22}H_{27}N_4}$ | $\mathrm{CoC_{23}H_{29}N_4}$ | $\mathrm{CoC_{23}H_{29}N_4}$ | $\mathrm{CoC_{24}H_{29}N_4O}$ |
| fw | 406.42 | 420.44 | 420.44 | 448.45 |
| cryst syst | monoclinic | orthorhombic | orthorhombic | orthorhombic |
| space group | $P2_1$ | *Pccn* | $Pca2_1$ | *Pbca* |
| *a*, Å | 10.533(6) | 31.260(7) | 8.547(2) | 19.222(2) |
| *b*, Å | 8.850(3) | 16.798(4) | 13.213(3) | 25.904(3) |
| *c*, Å | 11.293(9) | 7.661(5) | 17.724(4) | 8.517(1) |
| $\beta$, deg | 113.88(2) | | | |
| $V$, Å$^3$ | 963(1) | 4023(3) | 2002(2) | 4240.7(8) |
| $Z$ | 2 | 8 | 4 | 8 |
| $d_{\mathrm{calcd}}$, g/cm$^3$ | 1.402 | 1.388 | 1.395 | 1.405 |
| $T$, K | 225 | 225 | 200 | 202 |
| data collctn range, deg | $3 \leq 2\theta \leq 50$ | $3 \leq 2\theta \leq 44$ | $3 \leq 2\theta \leq 50$ | $3 \leq 2\theta \leq 50$ |
| data limits | $+h,+k,\pm l$ | $+h,+k,+l$ | $+h,+k,+l$ | $+h,+k,+l$ |
| no. of data collected | 2223 | 3474 | 3335 | 4369 |
| no. of unique data[a] | 1746 | 1502 | 1692 | 2600 |
| no. of parameters | 243 | 253 | 252 | 271 |
| $\mu$(Mo K$\alpha$), cm$^{-1}$ | 9.02 | 8.65 | 8.69 | 8.29 |
| transmission coeff | 0.95–1.00 | 0.86–1.00 | 0.89–1.00 | 0.88–1.00 |
| $R$[b] | 0.036 | 0.062 | 0.042 | 0.042 |
| $R_w$[c] | 0.040 | 0.051 | 0.047 | 0.049 |
| largest shift/esd, final | 0.043 | 0.061 | 0.027 | 0.017 |
| largest peak, e/Å≈3 | 0.35 | 0.46 | 0.41 | 0.45 |

[a] Observation criterion: $I > 3\sigma(I)$. [b] $R = \sum||F_o| - |F_c||/\sum|F_o|$. [c] $R_w = [\sum w(|F_o| - |F_c|)^2/\sum w|F_o|^2]^{1/2}$, where $w = 1/\sigma^2(F)$ and $\sigma^2(F)$ is defined in ref 19.

**Table II.** Final Positional Parameters for [CoEt(TC-3,3)][a]

| atom | *x* | *y* | *z* |
|---|---|---|---|
| Co | 0.20448(7) | 0.9881 | 0.67972(6) |
| N(1) | 0.3256(5) | 0.1176(5) | 0.6410(4) |
| N(2) | 0.1995(5) | 0.8883(5) | 0.5296(4) |
| N(3) | 0.0524(4) | 0.8837(5) | 0.6885(4) |
| N(4) | 0.1752(5) | 0.1123(5) | 0.8020(4) |
| C(1) | 0.3505(5) | 0.0843(7) | 0.5369(5) |
| C(2) | 0.4534(6) | 0.1519(7) | 0.5065(6) |
| C(3) | 0.4745(7) | 0.1506(8) | 0.3932(7) |
| C(4) | 0.4033(7) | 0.0767(8) | 0.2778(6) |
| C(5) | 0.2963(6) | 0.976(1) | 0.2537(5) |
| C(6) | 0.2386(6) | 0.9199(6) | 0.3341(5) |
| C(7) | 0.2631(5) | 0.9569(6) | 0.4631(5) |
| C(8) | 0.1241(6) | 0.7489(7) | 0.4758(6) |
| C(9) | 0.0942(7) | 0.6627(7) | 0.5761(6) |
| C(10) | −0.0046(6) | 0.7406(7) | 0.6214(6) |
| C(11) | −0.0108(5) | 0.9485(6) | 0.7556(5) |
| C(12) | −0.1434(6) | 0.9040(7) | 0.7454(5) |
| C(13) | −0.2239(6) | 0.9543(8) | 0.8090(6) |
| C(14) | −0.1921(7) | 0.0557(8) | 0.9092(7) |
| C(15) | −0.0686(7) | 0.1312(8) | 0.9676(6) |
| C(16) | 0.0453(6) | 0.1426(7) | 0.9361(6) |
| C(17) | 0.0695(6) | 0.0764(6) | 0.8338(5) |
| C(18) | 0.2678(7) | 0.2364(8) | 0.8701(7) |
| C(19) | 0.3141(7) | 0.3267(7) | 0.7812(7) |
| C(20) | 0.4024(7) | 0.2439(8) | 0.7259(6) |
| C(21) | 0.3607(6) | 0.8820(7) | 0.8132(5) |
| C(22) | 0.3308(8) | 0.801(1) | 0.9154(7) |

[a] Numbers in parentheses are errors in the last significant digit. Atoms are labeled as indicated in Figure 2.

**Table III.** Final Positional Parameters for [Co(*n*-Pr)(TC-3,3)][a]

| atom | *x* | *y* | *z* |
|---|---|---|---|
| Co | 0.60349(3) | 0.54071(5) | 0.0462(1) |
| N(1) | 0.5634(2) | 0.6221(3) | 0.1040(8) |
| N(2) | 0.5636(2) | 0.5221(3) | −0.1346(8) |
| N(3) | 0.6351(2) | 0.4460(3) | 0.0145(7) |
| N(4) | 0.6370(2) | 0.5470(3) | 0.2511(7) |
| C(1) | 0.5306(2) | 0.6325(4) | −0.005(1) |
| C(2) | 0.5030(2) | 0.6988(4) | 0.000(1) |
| C(3) | 0.4654(3) | 0.7142(4) | −0.089(1) |
| C(4) | 0.4428(3) | 0.6676(5) | −0.204(1) |
| C(5) | 0.4551(2) | 0.5929(5) | −0.2671(1) |
| C(6) | 0.4924(2) | 0.5514(4) | −0.238(1) |
| C(7) | 0.5290(2) | 0.5665(4) | −0.136(1) |
| C(8) | 0.5660(2) | 0.4573(4) | −0.262(1) |
| C(9) | 0.6119(2) | 0.4310(4) | −0.289(1) |
| C(10) | 0.6321(2) | 0.3917(4) | −0.133(1) |
| C(11) | 0.6592(2) | 0.4236(4) | 0.151(1) |
| C(12) | 0.6754(2) | 0.3456(4) | 0.173(1) |
| C(13) | 0.7009(2) | 0.3140(4) | 0.301(1) |
| C(14) | 0.7234(2) | 0.3489(4) | 0.433(1) |
| C(15) | 0.7229(2) | 0.4296(5) | 0.473(1) |
| C(16) | 0.6981(2) | 0.4901(4) | 0.407(1) |
| C(17) | 0.6651(2) | 0.4883(4) | 0.281(1) |
| C(18) | 0.6364(3) | 0.6145(4) | 0.370(1) |
| C(19) | 0.5911(3) | 0.6418(4) | 0.404(1) |
| C(20) | 0.5691(3) | 0.6772(4) | 0.248(1) |
| C(21) | 0.6406(2) | 0.6172(4) | −0.078(1) |
| C(22) | 0.6862(3) | 0.5944(4) | −0.107(1) |
| C(23) | 0.7125(3) | 0.6607(5) | −0.191(1) |

[a] Numbers in parentheses are errors in the last significant digit. Atoms are labeled as indicated in Figure 3.

empirical absorption correction was applied. The structure was solved and refined as described above for [CoEt(TC-3,3)]. Final coordinates for the non-hydrogen atoms are given in Table IV. Positional parameters for all atoms, anisotropic temperature factors, and all bond lengths and angles appear as Tables S7–S9 (supplementary material), respectively.

**[Co(COMe)(TC-4,4)].** A black plate-shaped crystal with approximate dimensions 0.04 × 0.25 × 0.42 mm was mounted as described above for [CoEt(TC-3.3)]. Open counter $\omega$-scans of low angle reflections revealed sharp ($\Delta\bar{\omega}_{1/2}$ = 0.22°) structureless profiles. The space group was determined to be *Pbca* (No. 61) from the systematic absences. The unit cell parameters were refined by using the setting angles of 25 reflections having $2\theta \geq 20°$. An empirical absorption correction was applied. The structure was solved and refined as described above for [CoEt(TC-3,3)]. Final coordinates for the non-hydrogen atoms are given in Table V. Positional parameters for all atoms, anisotropic temperature factors, and all bond lengths and angles appear as Tables S10–S12 (supplementary material), respectively.

## Results and Discussion

**The Synthesis and Structures of [CoR(TC-*n,m*)] Complexes. (a) [CoR(TC-3,3)].** Attempts to prepare cobalt alkyl tropocoronands began with the [TC-3,3]$^{2-}$ ligand since the structural analysis of [CoCl(TC-3,3)][11] revealed the [TC-3,3]$^{2-}$ macrocycle to adopt a nearly planar configuration, characteristic of coenzyme $\mathrm{B_{12}}$ and all of its models. Cobalamin model complexes are usually synthesized either by reduction of the Co(II) complex to Co(I) followed by addition of an electrophile or by oxidation of Co(II) to Co(III)–X and addition of a nucleophile.[20] Given the difficulty in obtaining large quantities of [CoCl(TC-3,3)], the [CoR(TC-3,3)] compounds were prepared by the Co(II) reduction route.

---

(20) Brown, K. L. In *B₁₂*; Dolphin, D., Ed.; John Wiley and Sons: New York, 1982; Vol. 1, pp 245–294.

**Table IV.** Final Positional Parameters for [CoMe(TC-4,4)][a]

| atom | *x* | *y* | *z* |
|---|---|---|---|
| Co | 0.02549(9) | 0.75438(8) | 0.7400 |
| N(1) | −0.0435(7) | 0.6722(4) | 0.6600(4) |
| N(2) | 0.1864(7) | 0.7793(5) | 0.6713(4) |
| N(3) | 0.1038(8) | 0.8282(5) | 0.8264(4) |
| N(4) | −0.1239(7) | 0.7130(5) | 0.8169(4) |
| C(1) | 0.056(1) | 0.6590(6) | 0.6025(5) |
| C(2) | 0.026(1) | 0.5934(7) | 0.5408(6) |
| C(3) | 0.113(1) | 0.5701(7) | 0.4783(5) |
| C(4) | 0.261(1) | 0.6011(6) | 0.4591(5) |
| C(5) | 0.353(1) | 0.6677(7) | 0.4969(6) |
| C(6) | 0.326(1) | 0.7199(6) | 0.5607(6) |
| C(7) | 0.197(1) | 0.7208(6) | 0.6111(5) |
| C(8) | 0.294(1) | 0.8661(7) | 0.6767(6) |
| C(9) | 0.4385(9) | 0.8409(7) | 0.7259(8) |
| C(10) | 0.393(1) | 0.7985(7) | 0.8019(6) |
| C(11) | 0.271(1) | 0.8659(8) | 0.8426(7) |
| C(12) | −0.003(1) | 0.8473(7) | 0.8784(5) |
| C(13) | 0.017(1) | 0.9260(6) | 0.9314(6) |
| C(14) | −0.069(1) | 0.9542(6) | 0.9938(5) |
| C(15) | −0.201(1) | 0.9105(7) | 0.0242(5) |
| C(16) | −0.276(1) | 0.8272(6) | 0.9944(6) |
| C(17) | −0.2558(9) | 0.7714(5) | 0.9299(5) |
| C(18) | −0.1365(8) | 0.7771(5) | 0.8750(5) |
| C(19) | −0.220(1) | 0.6211(7) | 0.8185(5) |
| C(20) | −0.156(1) | 0.5331(6) | 0.7714(5) |
| C(21) | −0.214(1) | 0.5323(6) | 0.6919(5) |
| C(22) | −0.203(1) | 0.6319(8) | 0.6557(5) |
| C(23) | −0.0975(9) | 0.8696(6) | 0.7071(4) |

[a] Numbers in parentheses are errors in the last significant digit. Atoms are labeled as indicated in Figure 4.

**Table V.** Final Positional Parameters for [Co(COMe)(TC-4,4)][a]

| atom | *x* | *y* | *z* |
|---|---|---|---|
| Co | 0.83181(2) | 0.37751(2) | 0.02683(6) |
| O(1) | 0.8573(2) | 0.4350(1) | −0.2344(3) |
| N(1) | 0.9081(2) | 0.3370(1) | −0.0420(4) |
| N(2) | 0.8849(2) | 0.3752(1) | 0.2200(4) |
| N(3) | 0.7613(1) | 0.4253(1) | 0.0834(4) |
| N(4) | 0.7587(1) | 0.3538(1) | −0.1123(3) |
| C(1) | 0.9611(2) | 0.3299(1) | 0.0550(4) |
| C(2) | 0.0192(2) | 0.2982(2) | 0.0192(5) |
| C(3) | 0.0797(2) | 0.2883(2) | 0.0990(6) |
| C(4) | 0.1022(2) | 0.3066(2) | 0.2445(6) |
| C(5) | 0.0652(2) | 0.3386(2) | 0.3432(6) |
| C(6) | 0.9994(2) | 0.3594(2) | 0.3278(5) |
| C(7) | 0.9493(2) | 0.3556(1) | 0.2078(4) |
| C(8) | 0.8611(2) | 0.3896(2) | 0.3795(5) |
| C(9) | 0.7829(2) | 0.3884(2) | 0.4014(5) |
| C(10) | 0.7456(2) | 0.4386(2) | 0.3680(5) |
| C(11) | 0.7698(2) | 0.4619(1) | 0.2133(4) |
| C(12) | 0.7032(2) | 0.4251(1) | −0.0005(4) |
| C(13) | 0.6463(2) | 0.4580(2) | 0.0342(5) |
| C(14) | 0.5833(2) | 0.4649(2) | −0.0390(5) |
| C(15) | 0.5562(2) | 0.4415(2) | −0.1736(5) |
| C(16) | 0.5886(2) | 0.4047(2) | −0.2631(5) |
| C(17) | 0.6525(2) | 0.3803(1) | −0.2428(5) |
| C(18) | 0.7036(2) | 0.3850(1) | −0.1248(4) |
| C(19) | 0.7563(2) | 0.3057(1) | −0.2051(5) |
| C(20) | 0.8029(2) | 0.2633(1) | −0.1430(5) |
| C(21) | 0.8767(2) | 0.2633(2) | −0.2086(5) |
| C(22) | 0.9098(2) | 0.3160(2) | −0.2030(5) |
| C(23) | 0.8698(2) | 0.4306(1) | −0.0965(5) |
| C(24) | 0.9201(2) | 0.4673(2) | −0.0170(5) |

[a] Numbers in parentheses are errors in the last significant digit. Atoms are labeled as indicated in Figure 8.

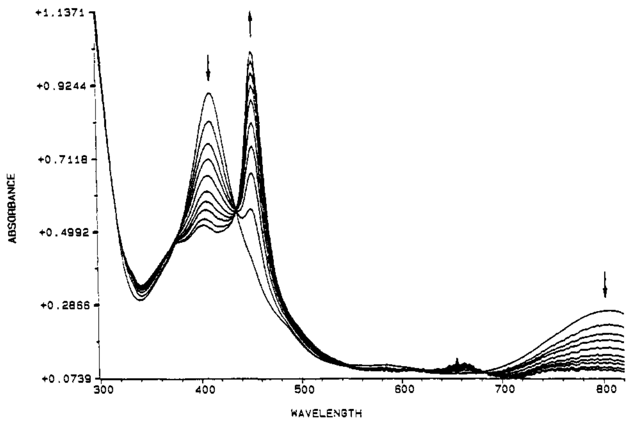

**Figure 1.** Conversion of a 2.5 × $10^{-5}$ M THF solution of [CoEt(TC-3,3)] to [Co(TC-3,3)] under the illumination of a simple flashlight. UV–visible spectra were recorded at 30-s intervals.

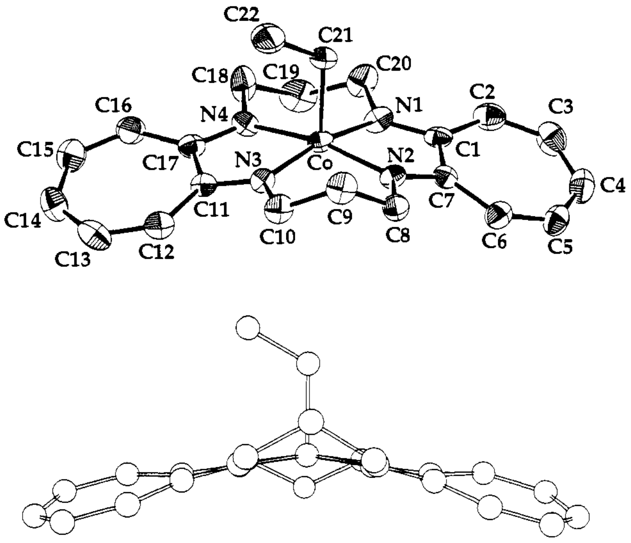

**Figure 2.** ORTEP drawing of the structure of [CoEt(TC-3,3)] showing the 50% thermal ellipsoids (top) for all non-hydrogen atoms. A PLUTO diagram depicting a side view is given at the bottom.

Following the general guidelines described by Costa,[21] green-black THF solutions of [Co(TC-3,3)] were reduced with 40% Na/Hg in about 10 min, resulting in vivid blue-green solutions presumed to contain the [Co(TC-3,3)]$^-$ anion, an extremely reactive intermediate which could not be isolated. The use of 1% Na/Hg or $NaBH_4$ in place of 40% sodium amalgam resulted in incomplete reduction. Filtration of the reduced solution followed by addition of EtBr or *n*-PrBr at −30 °C afforded crystalline [CoR(TC-3,3)] in low to moderate yields. This compound was also prepared in situ by using MeI as an electrophile, but pure product could not be isolated in this manner. Solutions of all the Co(III) tropocoronand alkyls are moderately light sensitive, as is the case for most $B_{12}$ models, and consequently were handled in darkness whenever possible. Figure 1 illustrates the electronic spectral changes that attend a typical decomposition of [CoEt(TC-3,3)] in THF solution under illumination from a simple flashlight, a procedure which cleanly affords [Co(TC-3,3)]. Studies of the rates of thermal decomposition are discussed in a later section.

The sharp proton solution NMR spectra of [CoEt(TC-3,3)] and [Co(*n*-Pr)(TC-3,3)] indicated the complexes to be diamagnetic, as is the case for all known Co(III) $B_{12}$ model complexes. Variable-temperature studies revealed fluxional behavior attributed to conformational equilibria of the methylene linker chains, as discussed in more detail elsewhere.[22] In order to obtain metrical information, X-ray diffraction studies were carried out on [CoEt(TC-3,3)] and [Co(*n*-Pr)(TC-3,3)]. The molecular structures are shown in Figures 2 and 3, respectively. Bond lengths and angles within the coordination sphere are listed in Tables VI and VII. The two complexes have similar solid-state structures, both exhibiting five-coordination with square-pyramidal geometry. The Co–C bond lengths of 1.963 (6) Å (Et) and 1.976 (7) Å (*n*-Pr)

---

(21) Costa, G.; Mestroni, G. *J. Organomet. Chem.* **1968**, *11*, 325.

(22) Jaynes, B. S. Ph.D. Thesis, Massachusetts Institute of Technology, 1992.

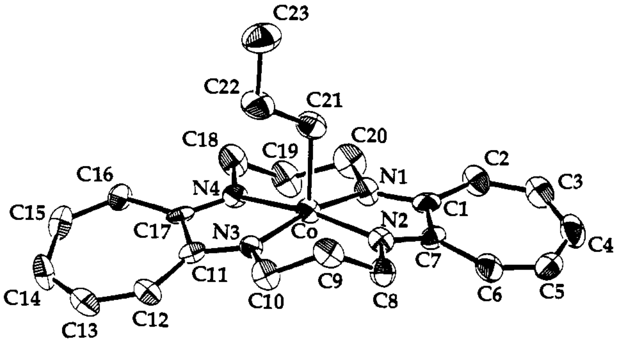

**Figure 3.** ORTEP drawing of the structure of [Co($n$-Pr)(TC-3,3)] showing the 50% thermal ellipsoids. Hydrogen atoms have been omitted.

**Table VI.** Bond Distances (Å) and Angles (deg) for the Coordination Sphere of [CoEt(TC-3,3)][a]

| | | | |
|---|---|---|---|
| | Bond Distances | | |
| Co–N1 | 1.893(5) | Co–N4 | 1.885(5) |
| Co–N2 | 1.893(5) | Co–C21 | 1.963(6) |
| Co–N3 | 1.887(4) | | |
| | Bond Angles | | |
| N1–Co–N2 | 81.5(2) | N2–Co–C21 | 100.1(2) |
| N1–Co–N3 | 167.1(2) | N3–Co–N4 | 81.5(2) |
| N1–Co–N4 | 98.1(2) | N3–Co–C21 | 101.0(2) |
| N1–Co–C21 | 91.9(2) | N4–Co–C21 | 92.9(2) |
| N2–Co–N3 | 95.9(2) | Co–C21–C22 | 116.7(4) |
| N2–Co–N4 | 167.0(2) | | |

[a] Atoms are labeled as indicated in Figure 2.

**Table VII.** Bond Distances (Å) and Angles (deg) for the Coordination Sphere of [Co($n$-Pr)(TC-3,3)][a]

| | | | |
|---|---|---|---|
| | Bond Distances | | |
| Co–N1 | 1.907(6) | Co–N4 | 1.891(6) |
| Co–N2 | 1.890(6) | Co–C21 | 1.976(7) |
| Co–N3 | 1.889(5) | | |
| | Bond Angles | | |
| N1–Co–N2 | 81.7(2) | N2–Co–C21 | 98.1(3) |
| N1–Co–N3 | 167.9(2) | N3–Co–N4 | 82.1(2) |
| N1–Co–N4 | 97.6(3) | N3–Co–C21 | 100.3(3) |
| N1–Co–C21 | 91.7(3) | N4–Co–C21 | 92.2(3) |
| N2–Co–N3 | 96.4(3) | Co–C21–C22 | 117.7(5) |
| N2–Co–N4 | 169.6(2) | | |

[a] Atoms are labeled as indicated in Figure 3.

are shorter than those of nearly all six-coordinate $B_{12}$ models,[23] and the Co(III) atom is raised above the plane of the nitrogen atoms by 0.19 and 0.21 Å, respectively. This upward displacement contrasts with that in six-coordinate Co alkyls, where the Co atom is usually displaced toward the axial base.

Although stable five-coordinate Co(III) alkyls exist in solution for both $B_{12}$ and $B_{12}$ model systems,[24] only three structurally characterized five-coordinate complexes in this family are known. The first, [Co($CH_3$)(acacen)], where acacen is the dianion of bis(acetylacetone)ethylenediimine, is a square-pyramidal structure with a Co–C bond length of 1.95(2) Å and the Co atom raised 0.12 Å above the plane of the nitrogen atoms.[25] The other two complexes, [CoMe(saloph)]·0.5$H_2O$ and [Co($i$-Pr)(saloph)·1.5$H_2O$, where saloph is the dianion of bis(salicylidene)-$o$-phenylenediamine, are also square pyramidal, with corresponding Co–C bond distances of 1.96(1) and 2.031(8) Å and Co atoms elevated above the planes of the nitrogen atoms by 0.11 and 0.16 Å, respectively.[24] The short Co–C bond distances and the displacement of the Co atom toward the alkyl are features that are shared with the Co(III) alkyl tropocoronands and suggest that these are general characteristics of five-coordinate Co(III) alkyls. Both effects can be explained by a stronger Co–C bonding interaction in the absence of a sixth ligand, which normally would compete with the alkyl for the metal $d_{z^2}$ orbital.

The factors that stabilize five-coordinate complexes are not fully understood, but it has been suggested that this coordination number is favored by electron-rich ligand systems. This hypothesis was supported by a study in which axial base exchange rates for [CoR(saloph)] compounds were compared to exchange rates for glyoxime model systems and cobalamins.[26] Whereas the saloph system is considered more electron rich than cobalamin, the glyoxime system is electron poor by comparison. The relative rates for glyoxime:cobalamin:saloph were $1:10^7:10^{10}$, respectively, demonstrating that the axial base is bound less tightly in the electron-rich systems. In the tropocoronand, potentially coordinating sixth ligands do not appear to bind strongly in solution. Addition of 1 equiv of pyridine to a toluene solution of [CoEt(TC-3,3)] gave a proton NMR spectrum that was unchanged from that of the starting material.

**(b) [CoR(TC-3,4)].** The solid-state geometry of the Co(III) halide complex [CoCl(TC-3,4)] is substantially distorted compared to that of [CoCl(TC-3,3)].[11] We therefore anticipated that similar structural differences might exist between [CoR(TC-3,3)] and [CoR(TC-3,4)]. Reduction of [Co(TC-3,4)] with 40% amalgam afforded the blue-green anion, as in the case of [Co(TC-3,3)], and addition of $n$-PrBr gave [Co($n$-Pr)(TC-3,4)] in moderate yield. Comparison of the proton NMR spectra of [Co($n$-Pr)(TC-3,3)] and [Co($n$-Pr)(TC-3,4)], however, revealed their solution state structures to be very similar. In particular, the chemical shifts of the propyl resonances are identical, indicating that the electronic environments of the two species are virtually the same.

Unfortunately, crystals suitable for an X-ray structural determination could not be grown. The UV–visible spectra, however, another measure of the electronic environment of the metal ion, again revealed the complexes to be structurally similar. Whereas the electronic spectra of [CoCl(TC-3,3)] and [CoCl(TC-3,4)] are qualitatively different, those of [Co($n$-Pr)(TC-3,3)] and [Co($n$-Pr)(TC-3,4)] are essentially the same. Both have an intense band at approximately 410 nm and a less intense, broad charge transfer band occurring at 796 nm for the former and at 825 nm for the latter.

**(c) [CoR(TC-4,4)].** Reduction of [Co(TC-4,4)] with 40% Na/Hg in THF resulted in the formation of a vivid blue-green color indicative of the $[Co(TC\text{-}4,4)]^-$ anion, but addition of EtBr or $n$-PrBr failed to yield a pure sample of the corresponding Co(III) alkyl. Impure [Co($n$-Pr)(TC-4,4)] could be prepared in situ at −78 °C, but the product quickly decomposed upon warming, as monitored by electronic spectroscopy. Addition of MeI to a solution of the anion, however, yielded substantial amounts of [CoMe(TC-4,4)], as determined spectroscopically, and the product was stable at room temperature in solution when protected from light.

The instability of the ethyl and propyl derivatives compared to the methyl derivative suggested that a decomposition pathway other than homolysis of the Co–C bond was available to the longer chain alkyls. One such possibility is $\beta$-hydride elimination, a reaction common to organometallic species.[27] Most $B_{12}$ models are resistant to $\beta$-hydride elimination by a conventional mechanism because the strongly binding planar $N_4$ ligand systems prevent the formation of a cis coordination site usually required for such reactions.[28] The flexible $[TC\text{-}4,4]^{2-}$ ligand, however, has already been shown to accommodate cis ligands in the six-coordinate [Co(acac)(TC-4,4)],[22] demonstrating that a $\beta$-hydride decom-

---

(23) Randaccio, L.; Pahor, N. B.; Zangrando, E.; Marzilli, L. G. *Chem. Soc. Rev.* **1989**, *18*, 225.

(24) Marzilli, L. G.; Summers, M. F.; Bresciani-Pahor, N.; Zangrando, E.; Charland, J.-P.; Randaccio, L. *J. Am. Chem. Soc.* **1985**, *107*, 6880.

(25) Bruckner, S.; Calligaris, M.; Nardin, G.; Randaccio, L. *Inorg. Chim. Acta* **1969**, *3*, 308.

(26) Summers, M. F.; Marzilli, L. G.; Bresciani-Pahor, N.; Randaccio, L. *J. Am. Chem. Soc.* **1984**, *106*, 4478.

(27) Collman, J. P.; Hegedus, L. S.; Norton, J. R.; Finke, R. G. *Principles and Applications of Organotransition Metal Chemistry*; University Science Books: Mill Valley, CA, 1987.

(28) An interesting recent investigation revealed that $\beta$-hydride elimination could occur from Ado/$Co^{II}$ radical pairs trapped in the solvent cage. See: Garr, C. D.; Finke, R. G. *J. Am. Chem. Soc.* **1992**, *114*, 10440.

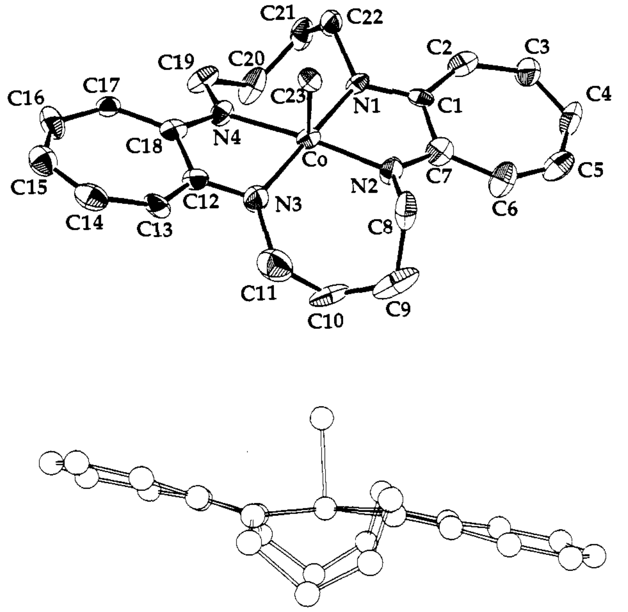

**Figure 4.** ORTEP drawing of the structure of [CoMe(TC-4,4)] showing the 50% thermal ellipsoids (top) for all non-hydrogen atoms and a side view (bottom) prepared with PLUTO.

**Table VIII.** Bond Distances (Å) and Angles (deg) for the Coordination Sphere of [CoMe(TC-4,4)][a]

| | | | |
|---|---|---|---|
| | Bond Distances | | |
| Co–N1 | 1.881(6) | Co–N4 | 1.945(6) |
| Co–N2 | 1.866(7) | Co–C23 | 1.940(8) |
| Co–N3 | 1.934(7) | | |
| | Bond Angles | | |
| N1–Co–N2 | 80.9(3) | N2–Co–N4 | 171.9(3) |
| N1–Co–N3 | 174.9(3) | N2–Co–C23 | 93.7(3) |
| N1–Co–N4 | 99.2(3) | N3–Co–N4 | 79.3(3) |
| N1–Co–C23 | 93.3(3) | N3–Co–C23 | 91.7(3) |
| N2–Co–N3 | 99.9(3) | N4–Co–C23 | 94.3(3) |

[a] Atoms are labeled as indicated in Figure 4.

position pathway is possible. The related reactivity of [CoMe(TC-4,4)] toward CO is discussed below.

Isolation of [CoMe(TC-4,4)] from the reaction of MeI with the Co(I) anion proved to be difficult, so alternative syntheses via the readily available [CoCl(TC-4,4)] complex[11] were developed. Addition of MeLi to a cold slurry of [CoCl(TC-4,4)] in THF resulted in [CoMe(TC-4,4)], contaminated with a small amount of [Co(TC-4,4)]. Crystallization of the product from a toluene/pentane mixture, however, afforded analytically pure material in moderate yield. Partial reduction of the halide to the Co(II) complex could be minimized by using MeMgBr in place of MeLi, but overall yields were somewhat lower. A proton NMR spectrum of the product revealed sharp resonances, clearly indicating that the product was diamagnetic.

The results of an X-ray structural study of [CoMe(TC-4,4)] are shown in Figure 4. In contrast to the unusual trigonal-bipyramidal structure found for the chloride analog [CoCl(TC-4,4)],[11] the methyl compound has square-pyramidal coordination geometry, similar to that of [CoR(TC-3,3)]. Bond lengths and angles within the coordination sphere are listed in Table VIII. The Co atom lies 0.11 Å above the plane of the nitrogen atoms and the Co–C bond length is only 1.940(8) Å. To our knowledge, this is the shortest structurally characterized Co–C(sp$^3$) bond. The Co–N distances are slightly asymmetric, with Co–N1 and Co–N2 at 1.881(6) and 1.866(7) Å and Co–N3 and Co–N4 at 1.934(7) and 1.945(6) Å, respectively. This distortion may result from C–C torsional strain within the linker chain, as discussed below.

**Table IX.** Torsion Angles, $\omega$ (deg), within the Linker Chains of [CoEt(TC-3,3)] and [CoMe(TC-4,4)][a]

| | | $\omega$ | $\lvert\Delta_{\mathrm{ideal}}\rvert$[b] |
|---|---|---|---|
| [CoEt(TC-3,3)] | | | |
| C–N | C1–N1–C20–C19 | 145.2(6) | 4.8 |
| | C7–N2–C8–C9 | 163.6(5) | 13.6 |
| | C9–C10–N3–C11 | –166.8(5) | 16.8 |
| | C17–N4–C18–C19 | –143.2(5) | 6.8 |
| C–C | C8–C9 | 66.3(6) | 6.3 |
| | C9–C10 | –64.2(7) | 4.2 |
| | C18–C19 | –64.8(8) | 4.8 |
| | C19–C20 | 63.7(8) | 3.7 |
| [CoMe(TC-4,4)] | | | |
| C–N | C1–N1–C22–C21 | 95.3(9) | 5.3 |
| | C7–N2–C8–C9 | –97.4(9) | 7.4 |
| | C10–C11–N3–C12 | 152.4(8) | 2.4 |
| | C18–N4–C19–C20 | –155.9(7) | 5.9 |
| C–C | C8–C9 | –52 (1) | 8 |
| | C9–C10 | –51(1) | 9 |
| | C10–C11 | 94 (1) | 34 |
| | C19–C20 | –90.6(9) | 30.6 |
| | C20–C21 | 48(1) | 12 |
| | C21–C22 | 54(1) | 6 |

[a] The sign of $\omega$ is positive if, when looking from atom 2 to atom 3, clockwise motion of atom 1 would superimpose it on atom 4. Atoms 1 and 4 are omitted for C–C angles. [b] $\Delta_{\mathrm{ideal}} = [|\omega| - \text{ideal angle}]$ where ideal angles are 30°, 90°, or 150° for C–N and 60° or 180° for C–C.

Geometric distortion is also evident when the side views of [CoMe(TC-4,4)] and [CoEt(TC-3,3)] are compared, as shown in Figures 2 and 4. Rather than adopting the symmetric downward bow-shaped (saddle) conformation of [CoR(TC-3,3)], the seven-membered tropone rings of the macrocycle in [CoMe(TC-4,4)] are now buckled in opposite directions with respect to the plane of the nitrogen atoms, one pointed upward and one downward. Such a buckling distortion positions the $\alpha$ and $\omega$ carbon atoms of the polymethylene linkers on opposite sides of the mean plane through the four-coordinated N atoms, thus increasing the distance between these chain terminii. The average $C_\alpha$ to $C_\omega$ distance for [CoEt(TC-3,3)] is 2.54 Å, whereas the average for [CoMe(TC-4,4)] is 2.92 Å. In the [CoCl(TC-*n*,*m*)] complexes, a distortion toward trigonal-bipyramidal geometry resulted in an increased average $C_\alpha$ to $C_\omega$ distance of 0.57 Å upon moving from [CoCl(TC-3,3)] to [CoCl(TC-4,4)].

The torsion angles, $\omega$ (deg), for bonds within the methylene linker chains of [CoEt(TC-3,3)] and [CoMe(TC-4,4)] are collected in Table IX. Strain energies of metal chelating diamine ligands depend almost exclusively on C–C bond torsion angles rather than on the actual conformation of the ring.[29] Expanding this analysis to the tropocoronand linker chain chelate rings, the deviations of $\omega$ from their ideal values should approximate the degree of strain within the complex. Ideal $\omega$ values are 60° or 180° for C(sp$^3$)–(sp$^3$), whereas those for C(sp$^3$)–N(sp$^2$) are 30°, 90° or 150°.[30] Deviations from these values, $|\Delta_{\mathrm{ideal}}|$, are also listed in the table. The maximum deviation for a C–C torsion angle in [CoEt(TC-3,3)] is only 6.3°, suggesting that the complex has very little torsional strain. By contrast, [CoMe(TC-4,4)] contains two C–C bonds in the linker chains with $|\Delta_{\mathrm{ideal}}|$ values of greater than 30°, the largest found in any of the cobalt tropocoronands. Consequently, the torsional strain energy of the seven-membered chelate rings of [CoMe(TC-4,4)] is high compared to the six-membered rings of [CoEt(TC-3,3)].

**Factors Determining the Choice of Trigonal-Bipyramidal vs Square-Pyramidal Geometry.** Both [CoCl(TC-4,4)] and [CoMe(TC-4,4)] are distorted with respect to their [TC-3,3]$^{2-}$ and [TC-3,4]$^{2-}$ analogs in order to alleviate increased torsional strain in the methylene linker chains. Nevertheless, the molecules adopt completely different geometries to achieve this end. In the case of the cobalt alkyl, the buckling of the tropocoronand ligand appears to be a less efficient way of reducing this strain, since the average $C_\alpha$–$C_\omega$ distance increases by only 0.38 Å compared

---

(29) Hawkins, C. J. *Absolute Configuration of Metal Complexes*; John Wiley and Sons: New York, 1971.

(30) Bailey, M. F.; Maxwell, I. E. *J. Chem. Soc., Dalton Trans.* **1972**, 938.

to 0.57 Å in the halide complexes, upon moving from $[\mathrm{TC}\text{-}3,3]^{2-}$ to $[\mathrm{TC}\text{-}4,4]^{2-}$. Consequently, substantial torsional strain remains in the linker chains, as discussed above. The stabilization that balances this torsional strain must arise from the Co–Me bond. The methyl carbon is a strong $\sigma$-donor in comparison to chloride ion, and this $\sigma$-donation is better accommodated by the metal $d_{z^2}$ orbital, which points directly toward the alkyl in a square-pyramidal configuration. Thus, in [CoMe(TC-4,4)] there is a tradeoff whereby a higher energy ring conformation occurs, affording a stereochemical orientation at the metal where a stronger Co–C bond can form. The chloride ion, a relatively weak $\sigma$-donor by comparison, has less need for a $\sigma$-directed bonding orbital and enables the [CoCl(TC-4,4)] complex to adopt the conformationally less strained trigonal-bipyramidal stereochemistry, in which the $d_{xy}$ and $d_{x^2-y^2}/(p_x,p_y)$ orbitals are available for bonding, instead of the $d_{z^2}/(p_z)$.[11]

In order to evaluate this hypothesis, MO calculations using the X$\alpha$ method were carried out to compare the orbital bonding energies of a square-pyramidal alkyl with a hypothetical trigonal-bipyramidal alkyl species in which the alkyl is located in an equatorial position. To reduce computation time, the tropocoronand ligand was replaced by four amide ligands, $NH_2^-$, which maintain the trigonal geometry and provide the lone pairs of the tropocoronand nitrogen donor atoms. Calculations were performed on $[\mathrm{CoMe(NH_2)_4}]^{2-}$ in both square-pyramidal and trigonal-bipyramidal stereochemistries, using bond lengths and angles determined from the X-ray diffraction studies where applicable, with slight adjustments to give idealized geometry. The orientation of the $NH_2^-$ plane is very important in determining the splitting pattern of the d orbitals, and it was fixed in such a manner as always to contain the Co atom and lie perpendicular to the N–Co–C(alkyl) plane.

The results for the hypothetical trigonal-bipyramidal structure are shown in the form of a molecular orbital energy level diagram in Figure 5a, and Table S13 (supplementary material) summarizes the composition and energies of the valence molecular orbitals. The metal-based orbitals are, in ascending order of energy, 8a″ ($d_{xz}$), 14a′ ($d_{yz}$), 9a″ ($d_{xy}$, HOMO), 15a′ ($d_{x^2-y^2}$, LUMO), and 16a′ ($d_{z^2}$). The HOMO ($d_{xy}$) is separated from the LUMO ($d_{x^2-y^2}$) by 0.59 eV. Compared with the results for the corresponding halide model,[11] the energy levels of the d-block orbitals are raised owing to the reduced effective charge on the Co center. The separation between the HOMO and $d_\pi$ orbitals ($d_{xz,yz}$) is diminished because the latter are destabilized by an antibonding interaction with the $NH_2^-$ lone pair. The $d_{z^2}$ orbital remains the highest energy d orbital. The significant difference is that the order of frontier orbitals observed for the halide model is inverted in the alkyl analog, apparently due to increased $\sigma$-donation from C to the $d_{x^2-y^2}$ orbital ($CH_3^-$ is a much stronger base than $Cl^-$), and the synergetic elimination of $\pi$-donation from the lone pair of $Cl^-$ to the $d_{xy}$ orbital.

Turning to the square-pyramidal case shown in Figure 5b and Table S14 (supplementary material) the metal-based orbitals were found to be 11a′ ($d_{z^2}$, Co–C $\sigma$-bonding, not shown), 8a″ ($d_{xy}$), 9a″ and 14a′ ($d_{xz,yz}$), 15a′ ($d_{z^2}$, Co–C $\sigma$-antibonding), and 16a′ ($d_{x^2-y^2}$). Although this order is identical to that found for the corresponding halide compound,[11] the energy gap between the pseudodegenerate HOMO ($d_{xz}$ and $d_{yz}$) and the LUMO ($d_{z^2}$) is dramatically increased, from 0.19 to 1.16 eV. It is also interesting to note that this gap is nearly twice that of the hypothetical trigonal-bipyramidal structure. The larger gap between the HOMO and LUMO for the square-pyramidal case is strong evidence for its greater stability and provides a theoretical understanding of the experimental observations. In addition, the large calculated HOMO-LUMO gap agrees with the observation that all of the cobalt alkyls are diamagnetic, whereas the halides, predicted to have very small HOMO-LUMO gaps, are paramagnetic.[11]

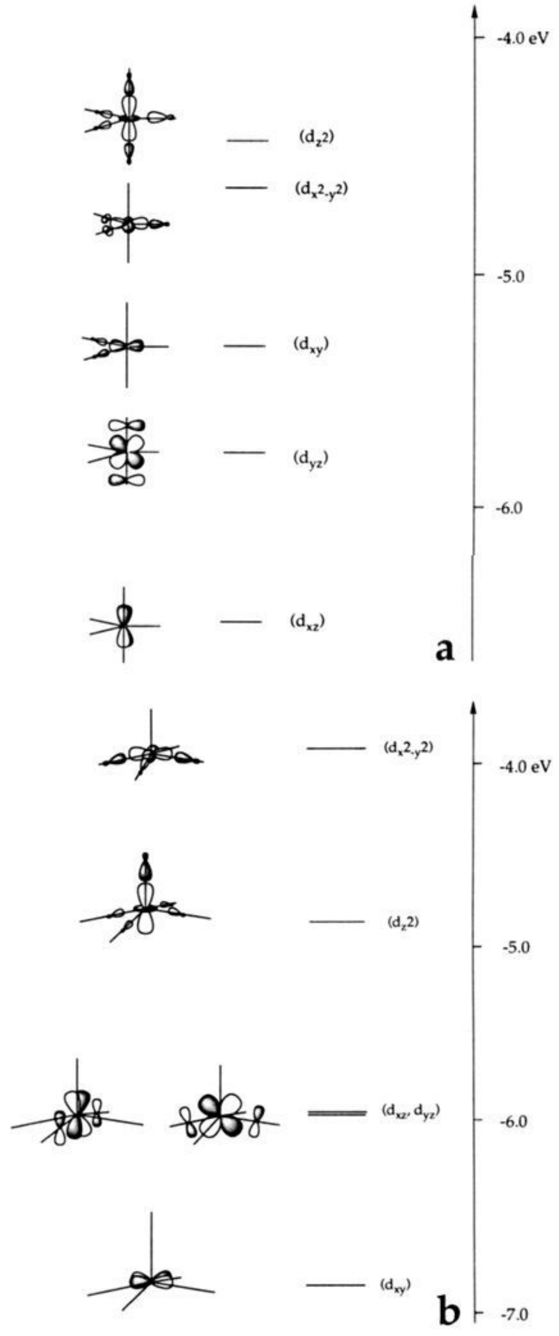

**Figure 5.** Calculated molecular orbital energy level diagram for (a, top) trigonal-bipyramidal and (b, bottom) square-pyramidal $[\mathrm{CoMe(NH_2)_4}]^{2-}$.

**Alkyl Radical Trapping Experiments.** In order to investigate the possibility that the Co(III) alkyls decompose by a homolytic pathway in solution, several radical trapping experiments were carried out by employing the radical trap, 2,2,6,6-tetramethylpiperidine-1-oxyl (TEMPO), shown below. The use of TEMPO as a radical trap in Co alkyl systems was pioneered by Finke[31] because of its relative stability and lack of redox chemistry with Co(II). Reaction of an alkyl radical R• with TEMPO gives the resulting trapped product R(TEMPO) at essentially diffusion controlled rates. Since cobalt–alkyl homolyses are generally

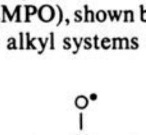

TEMPO

---

[31] Finke, R. G.; Smith, B. L.; Mayer, B. J.; Molinero, A. A. *Inorg. Chem.* **1983**, *22*, 3677.

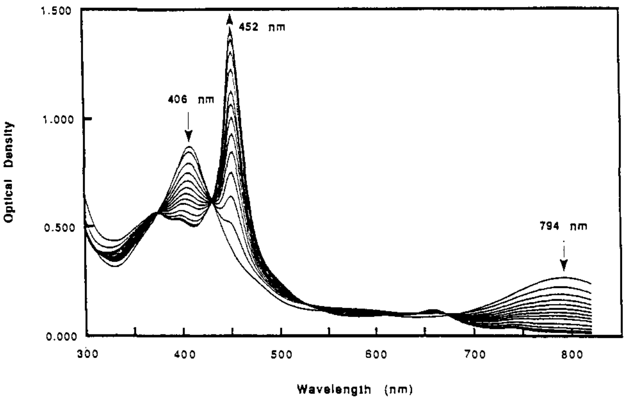

Figure 6. UV–visible spectra monitoring the conversion of a $2.9 \times 10^{-5}$ M THF solution of [CoMe(TC-3,3)] to [Co(TC-3,3)] at 40 °C in darkness, with a 181-fold excess of TEMPO. The total elapsed time is 17 000 s.

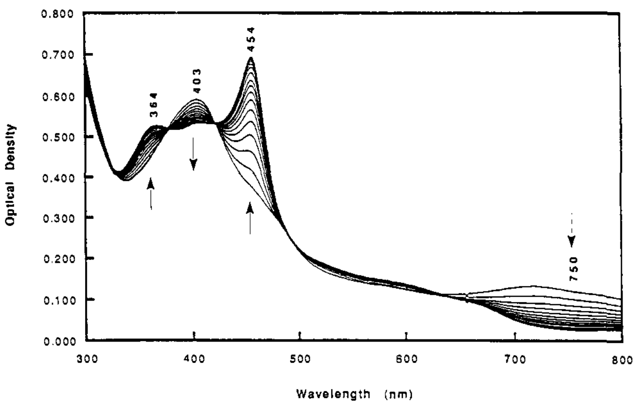

Figure 7. UV–visible spectra monitoring the conversion of a $2.9 \times 10^{-5}$ M THF solution of [CoMe(TC-4,4)] to [Co(TC-4,4)] at 40 °C in darkness, with a 181-fold excess of TEMPO. The total elapsed time is 3200 s.

reversible reactions, large excesses of TEMPO (25–200-fold) are usually used in order to eliminate recombination of R$^{\bullet}$ and Co(II), resulting in first-order rate laws.[32]

**(a) [CoMe(TC-3,3)].** A solution of [CoMe(TC-3,3)] was prepared from [Co(TC-3,3)]$^{-}$ and MeI in THF at −78 °C. To this solution was slowly added a THF solution of TEMPO (10-fold excess) and ferrocene (internal standard), following which the reaction was warmed to 50 °C for 2 h in order to homolyze the Co–C bond. These conditions were adopted to mimic those of the kinetics measurements described in the next section. A GC analysis of the resulting solution revealed a 37% yield of MeTEMPO when compared with an authentic sample prepared by addition of MeMgBr to TEMPO. The relatively low yield of trapped radical may result from incomplete formation of [CoMe(TC-3,3)] in the initial alkylation or other unidentified decomposition pathways. No other major products were visible in the GC traces, however.

**(b) [CoMe(TC-4,4)].** A solution of crystalline [CoMe(TC-4,4)], ferrocene, and a 10-fold excess of TEMPO was prepared in the dark in THF and then warmed to 50–55 °C for 2 h. GC analysis of the resulting solution, using calibration as described above for [CoMe(TC-3,3)], indicated a yield of 33% MeTEMPO. The low yield of MeTEMPO is not fully understood, but, as discussed for [CoMe(TC-3,3)], it may result from side reactions having products that are not detectable by GC.

**Preliminary Kinetic Analysis of the Homolysis Reactions.** Of primary interest in cobalamin and cobalamin model studies is the determination of relative rates of bond homolysis. Rate studies at various temperatures have now been used by several research groups to measure activation parameters for the Co–C bond.[5,6,31–34] We initiated a kinetic study of the homolysis of the cobalt alkyl tropocoronands to compare the relative rates of Co–C bond-breaking in [CoR(TC-3,3)] versus [CoR(TC-4,4)]. In order to evaluate the effects of the ligand constraints on this rate, the comparison was made between [CoMe(TC-3,3)] and [CoMe(TC-4,4)], complexes with identical alkyl groups.

Spectra for kinetic runs at 40 °C are shown in Figures 6 and 7 for [CoMe(TC-3,3)] and [CoMe(TC-4,4)], respectively. The presence of isosbestic points indicates clean conversion from the alkyl to the Co(II) species. Kinetic traces at 406, 452, and 794 nm for [CoMe(TC-3,3)], and at 400, 454, and 750 nm for [CoMe(TC-4,4)], were fit to equations corresponding to first-order decay of the alkyls and buildup for the Co(II) complexes. First-order rate constants of $1.5 \times 10^{-4}$ s$^{-1}$ for [CoMe(TC-3,3)] and $1.9 \times 10^{-3}$ s$^{-1}$ for [CoMe(TC-4,4)] were obtained. Thus, at 40 °C in THF, the homolysis of the Co–C bond is approximately 13 times faster for [CoMe(TC-4,4)] than for [CoMe(TC-3,3)].

The significantly faster homolysis observed for [CoMe(TC-4,4)] may indicate that internal strain or steric interactions are weakening the Co–C bond with respect to that in [CoMe(TC-3,3)]. One potential source of strain in the complex is the torsion angles between atoms C10 and C11, and C19 and C20, as discussed earlier, which deviate by more than 30° from their idealized values. A more complete kinetic study, in which activation parameters and bond dissociation energies are measured, is planned in order to evaluate further the factors that differentiate the reactivity of the two compounds.

**Insertion Reactions of [CoR(TC-*n*,*n*)].** The strongly coordinating planar $N_4$ macrocycles such as those in the cobalamins and their model complexes generally prevent any two additional ligands from binding in cis positions. Consequently, migratory insertion reactions by a classical cis coordination site mechanism are not observed in these systems.[27] Apparent insertion of CO into a cobalamin Co–C bond was observed in one case,[35] but the reaction was shown actually to occur via the generation of an alkyl radical that was subsequently trapped by CO. Irradiation of an aqueous methylcobalamin solution under 31 atm of CO gave the acetylcobalamin in 65% yield after 2 h. The dependence of the reaction on photolytic conditions as well as high pressures of CO confirmed that it proceeded by a radical process rather than by a classical insertion pathway.

Given the considerable flexibility of the tropocoronand ligand demonstrated in the synthesis of the Co(III) halides[11] and the six-coordinate [Co(acac)(TC-4,4)],[22] we were interested in examining possible insertion reactions with the corresponding Co(III) alkyls. The addition of 1–2 atm of CO to a toluene solution of [CoMe(TC-4,4)] resulted in the gradual decay of the alkyl resonances over 30 min at 40 °C, as monitored by NMR spectroscopy, and the formation of new resonances corresponding to the CO-inserted product, [Co(COMe)(TC-4,4)]. The latter was isolated in moderate yield by preparing [CoMe(TC-4,4)] in situ in toluene from [CoCl(TC-4,4)] and then stirring the solution in darkness under 1–2 atm of CO for 1 h. Filtration and addition of pentane, followed by cooling to −30 °C, gave a black crystalline air-stable solid. Solutions of the acyl complex were stable indefinitely under inert atmosphere protected from light and showed no tendency to lose CO.

The IR spectrum of solid [Co(COMe)(TC-4,4)] contains an intense stretching frequency at 1685 cm$^{-1}$ corresponding to the inserted CO functionality. A CO stretching frequency was not reported for the acylcobalamin reported above, but the corresponding band in the $B_{12}$ model complex [Co(COMe)(acacen)], where acacen is the dianion of bis(acetylacetone)ethylenediimine, prepared from the acetyl chloride, occurs at 1720 cm$^{-1}$. In $[(ClO_4)LCoC(O)CH_3](ClO_4)$, L = [14]aneN$_4$, the band occurs

---

[32] Hay, B. P.; Finke, R. G. *Polyhedron* **1988**, *7*, 1469.

[33] Hay, B. P.; Finke, R. G. *J. Am. Chem. Soc.* **1986**, *108*, 4820.

[34] Tsou, T.-T.; Loots, M.; Halpern, J. *J. Am. Chem. Soc.* **1982**, *104*, 623.

[35] Krautler, B. *Helv. Chim. Acta* **1984**, *67*, 1053.

at 1695 cm$^{-1}$.[36] The NMR spectrum of [Co(COMe)(TC-4,4)] indicates that the inserted product remains five-coordinate, as in the parent complex, since the only major change in the spectrum is the downfield shift of the methyl resonance from 1.77 to 2.09 ppm. The possibility that the acyl group is coordinated in an $\eta^2$ fashion is eliminated by the relatively high CO stretching frequency. Typically, $\eta^2$-acyls have stretching frequencies in the range 1460–1620 cm$^{-1}$ as a result of the lower C–O bond order, and they generally occur in the earlier, more oxophilic transition metals.[27]

In contrast to the reaction of [CoMe(TC-4,4)], when 1–2 atm of CO was added to a toluene solution of [CoEt(TC-3,3)] no change was observed in the proton NMR spectrum after heating for 30 min at 50 °C. Although the ethyl derivative was employed in this case, previous studies have determined that CO insertion is generally faster for M–Et than for M–Me bonds.[27] Therefore, the inability of CO to insert into the Co–Et bond of [CoEt(TC-3,3)] can be attributed to the altered steric constraints of the ligand rather than the use of a different alkyl group. Apparently, the reduced flexibility of the [TC-3,3]$^{2-}$ in comparison to [TC-4,4]$^{2-}$ shuts down the insertion pathway by prohibiting the requisite coordination of CO cis to the alkyl.

CO insertion reactions generally proceed via the two-step mechanism shown in eq 2.[27] CO coordinates in the first step,

$$L_4M(CO)R \rightarrow L_4M(COR) \tag{2}$$

$$L_4M(COR) + L \rightarrow L_5M(COR)$$

followed by alkyl migration to produce the unsaturated acyl intermediate, which in turn is trapped by another ligand, L. In most cases, the acyl intermediate is unstable and cannot be isolated unless the carbonyl binds in an $\eta^2$ fashion. Five-coordinate sixteen-electron intermediates of the type [RhCl$_2$(PPh$_3$)$_2$] have been obtained by oxidative addition of acyl halides to [RhCl(PPh$_3$)$_3$], but these often exist in equilibrium in solution with the six-coordinate [RhRCl$_2$(CO)(PPh$_3$)$_2$] species, in which the alkyl has migrated to the open coordination site.[37] The sixteen-electron [Co(COMe)(TC-4,4)] complex appears to be an unusual example of a stable five-coordinate CO-inserted "intermediate" which shows no tendency to deinsert despite the fact that a potential open coordination site exists adjacent to the acyl. An alternative mechanism to migratory insertion would involve Co–C bond homolysis followed by reaction of the alkyl radical with CO to form the acyl radical and recombination to give the acyl complex. This sequence has recently been demonstrated for photochemical CO insertion into the Co–C bond of [(H$_2$O)LCoCH$_3$]$^{2+}$.[36] Since we do not observe an insertion product for [CoEt(TC-3,3)], such an alternative mechanism seems less likely, but kinetics studies are planned to investigate this possibility further.

An X-ray structural study was carried out on [Co(COMe)(TC-4,4)] in order to obtain detailed information about the coordination geometry. The molecular structure, shown in Figure 8, consists of a five-coordinate Co atom, as anticipated. Bond lengths and angles for the coordination sphere are listed in Table X. The Co–C bond length is only 1.878 (4) Å, slightly shorter than that of 1.89(1) Å found in another Co–C(sp$^2$) complex, [Co(CH=CH$_2$)(acacen)(H$_2$O)].[38] This extremely short bond apparently results, in part, from $\pi$-bonding interactions between the metal $d_{xz}$ and $d_{yz}$ orbitals and the $\pi^*$ orbital of the carbonyl group. The unusually short Co–C bond in the vinyl complex mentioned above was attributed to partial double bond character between the metal and the vinyl carbon atom. In the present case, $\pi$-back-donation is manifest by alignment of the acyl group approximately along the Co–N4 bond axis, the O–C23–Co–N1 and O–C23–Co–N4 torsion angles being 85.9(4) and -14.9(4)°, respectively. Similar bond shortening is observed in Co alkyls that are substituted with electron-withdrawing halogen atoms.[39–41] In two recently reported six-coordinate complexes, [(ClO$_4$)LCoC(O)CH$_3$](ClO$_4$) and [(H$_2$O)LCoC(O)CH$_3$](ClO$_4$)$_2$·H$_2$O, the Co–C bond lengths are 1.929(2) and 1.911(2) Å, respectively.[36] The longer distances in these complexes compared to [Co(COMe)(TC-4,4)] are attributed to their higher coordination number.

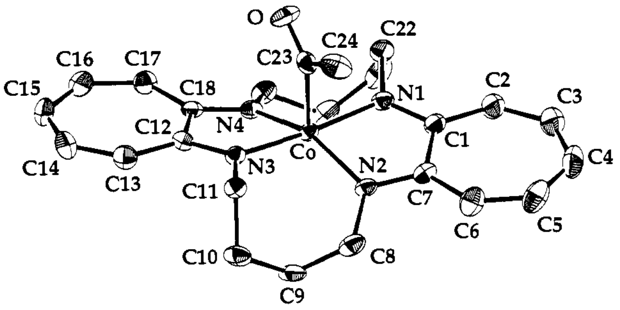

**Figure 8.** ORTEP drawing of [Co(COMe)(TC-4,4)] showing the 50% thermal ellipsoids for all non-hydrogen atoms.

**Table X.** Bond Distances (Å) and Angles (deg) for the Coordination Sphere of [Co(COMe)(TC-4,4)][a]

| | | | |
|---|---|---|---|
| | Bond Distances | | |
| Co–N1 | 1.896(3) | Co–C23 | 1.878(4) |
| Co–N2 | 1.937(3) | C23–O | 1.204(5) |
| Co–N3 | 1.897(3) | C23–C24 | 1.516(5) |
| Co–N4 | 1.939(3) | | |
| | Bond Angles | | |
| N1–Co–N2 | 80.7(1) | N2–Co–C23 | 107.0(2) |
| N1–Co–N3 | 172.7(1) | N3–Co–N4 | 81.0(1) |
| N1–Co–N4 | 101.3(1) | N3–Co–C23 | 86.7(1) |
| N1–Co–C23 | 86.1(1) | N4–Co–C23 | 99.9(1) |
| N2–Co–N3 | 100.4(1) | Co–C23–O | 122.5(3) |
| N2–Co–N4 | 153.1(1) | Co–C23–C24 | 117.2(3) |

[a] Atoms are labeled as indicated in Figure 8.

In contrast to [CoR(TC-3,3)] and [CoMe(TC-4,4)], the coordination geometry of the acyl is significantly distorted away from square pyramidal toward trigonal bipyramidal. The N1–Co–N3 bond angle is nearly linear, 172.7(1)°, but the N2–Co–N4 angle is 153.1(1)°, which lies between the expected values of a square pyramid (168°) and a trigonal bipyramid (120°). Interestingly, the average $C_\alpha$-to-$C_\omega$ distance in the linker chains is 2.95 Å, roughly the same as that found in [CoMe(TC-4,4)], indicating that substantial torsional strain still exists in the linker chains, despite the distortion. This strain is confirmed by the C–C torsion angles of -90.8(4)° for C8–C9 and -89.7(4)° for C19–C20, both deviating approximately 30° from their ideal values. Distortion toward trigonal-bipyramidal geometry was previously observed only in the Co halide tropocoronand complexes, which do not require a strong $\sigma$-bonding orbital for the Co–X bond. The trigonal-bipyramidal distortion of the acyl complex suggests that the reduced electron donating properties of the acyl, compared to an alkyl, lessens the requirement for bonding to the $d_{z^2}$ orbital and allows the complex to adopt a configuration on the pathway between square-pyramidal and trigonal-bipyramidal geometry. Further investigation of the ability of ligand (L) donor strength to tune the stereochemistry of [CoL(TC-*n*,*m*)] complexes is in progress.

---

(36) Bakac, A.; Espenson, J. H.; Young, V. G., Jr. *Inorg. Chem.* **1992**, *31*, 4959.

(37) Slack, D. A.; Egglestone, D. L.; Baird, M. C. *J. Organomet. Chem.* **1978**, *146*, 71.

(38) Bruckner, S.; Calligaris, M.; Nardin, G.; Randaccio, L. *Inorg. Chim. Acta* **1968**, *2*, 416.

(39) Chen, Q.; Marzilli, L. G.; Pahor, N. B.; Randaccio, L.; Zangrando, E. *Inorg. Chim. Acta* **1988**, *144*, 241.

(40) Toscano, P. J.; Konieczny, L.; Liu, S.; Zubieta, J. *Inorg. Chim. Acta* **1989**, *166*, 163.

(41) Toscano, P. J.; Brand, H.; Liu, S.; Zubieta, J. *Inorg. Chem.* **1990**, *29*, 2101.

## Conclusions

A family of Co(III) alkyl complexes has been synthesized by using the macrocyclic tropocoronand ligands. [CoEt(TC-3,3)], [Co(*n*-Pr)(TC-3,3)], and [CoMe(TC-4,4)] have similar five-coordinate square-pyramidal coordination geometries, the structures of which differ from those of the corresponding Co(III) halides, which are strongly dependent on the size of the macrocycle. This difference is a consequence of the strong $\sigma$-donor character of the alkyl groups, which bind preferentially to the $d_{z^2}$ orbital in square-pyramidal coordination. The Co alkyls all homolyze to give the corresponding Co(II) complex, and thus serve as model systems for coenzyme $B_{12}$. Alkyl radicals generated in the homolysis of [CoMe(TC-3,3)], [Co(*n*-Pr)(TC-3,3)], and [CoMe(TC-4,4) were trapped by using TEMPO. The homolysis rates of the methyl complexes were investigated and found to be significantly faster for [CoMe(TC-4,4)] than for [CoMe(TC-3,3)]. The increased rate of [CoMe(TC-4,4)] may be a result of torsional strain within the macrocycle, which is evident in the solid-state structure.

Facile insertion of CO into the Co–C bond of [CoMe(TC-4,4)] was discovered, in contrast with [CoEt(TC-3,3)] which failed to insert CO. The difference in reactivity is ascribed to the different ligand sizes, $[TC\text{-}4,4]^{2-}$ providing enough flexibility to allow cis coordination of the alkyl and CO, while $[TC\text{-}3,3]^{2-}$ does not. A structure determination of [Co(COMe)(TC-4,4)] revealed the Co–C bond to be extremely short, 1.878(4) Å, and the coordination geometry to distort from square pyramidal toward trigonal bipyramidal. The sharp contrast in reactivity between [CoR(TC-3,3)] and [CoR(TC-4,4)] demonstrates how twists in the geometry of the ligand can alter reactivity at the metal center.

**Acknowledgment.** This work was supported by a grant from the National Science Foundation. We are grateful to the George R. Harrison Spectroscopy Laboratory for allowing access to their facility supported by NSF (CHE-8914953) and NIH (P41RR02594). A. Masschelein thanks N.A.T.O. and C.I.E.S. for fellowships.

**Supplementary Material Available:** Tables of atomic positional parameters for all atoms, anisotropic temperature factors, bond distance and angles for all structurally characterized compounds, and upper valence molecular orbitals for two model stereochemistries (25 pages). Ordering information is given on any current masthead page.